JOURNAL OF CATALYSIS 55, 166–177 (1978)

# The Hydrogen–Oxygen Reaction on Lanthanide Oxides

## VII. The Hydrogen–Oxygen Reaction on Samarium Oxide

JOHN F. READ, YUK TONG CHAN, AND REID E. CONRAD

*Department of Chemistry, Mount Allison University, Sackville, New Brunswick, Canada EOA 3CO*

Received December 23, 1977; revised May 30, 1978

The stoichiometric hydrogen–oxygen reaction has been studied over samarium oxide at an approximately constant initial hydrogen pressure of 220 $N$ m$^{-2}$ over the temperature range 323 to 558 K and at varying initial hydrogen pressures at six different temperatures. The nonstoichiometric reaction has been studied at hydrogen–oxygen ratios from 0.14 to 10.2, at initial hydrogen pressures up to about $1 \times 10^3$ $N$ m$^{-2}$, and at 423, 500, 589, and 650 K. After detailed kinetic analysis it appears that the results best fit an equation of the form:

$$-\frac{dP_{\mathrm{T}}}{dt} = \frac{kb_{\mathrm{H}_2}{}^2P_{\mathrm{H}_2}{}^2b_{\mathrm{O}_2}P_{\mathrm{O}_2}}{(1 + b_{\mathrm{H}_2}P_{\mathrm{H}_2} + b_{\mathrm{O}_2}P_{\mathrm{O}_2})^3},$$

where $k$ is a proportionality constant, $b_{\mathrm{H}_2}$ and $b_{\mathrm{O}_2}$ are the adsorption coefficients for hydrogen and oxygen, respectively, $P_{\mathrm{T}}$ is the total pressure of hydrogen plus oxygen, and $P_{\mathrm{H}_2}$ and $P_{\mathrm{O}_2}$ are the partial pressures for hydrogen and oxygen, respectively. The most likely mechanism is one involving the competitive adsorption of molecular hydrogen and oxygen, with the rate-determining step involving the interaction between $H_2O_{2(\mathrm{ads})}$ and $H_{2(\mathrm{ads})}$.

## INTRODUCTION

Samarium oxide has been used effectively as a catalyst, particularly in organic oxidation reactions, since 1930 (*1*). A significant amount of this research has been summarized by Minachev (*2*), who relates the low to intermediate activity of samarium oxide within the lanthanide oxides to its electronic structure. Hattori *et al.* (*3*) have developed this concept and related the activity toward the oxidation of butane to the fourth ionization potential from the normal 3+ to the 4+ state.

Oxygen exchange has been studied extensively; see, for example, (*4–6*). Winter (*6*) notes that the rate-determining step is the desorption of molecular oxygen. The activity of samarium oxide depends critically on pretreatment. The activation energy is reported as 76 kJ mol$^{-1}$ on an oxygen-pretreated sample (*6*) and 48 kJ mol$^{-1}$ on a sample heated in air and then *in vacuo* (*4*). Sokolovskii *et al.* (*5*) compared the activity of an oxygen-pretreated sample with one that was just heated *in vacuo* and noted a decrease in activity after oxygen pretreatment below 450 K, but no difference above this temperature. They attribute this to the high mobility of oxygen above 450 K. Other oxidation reactions also illustrate the dependence of activity on surface conditions. For example, the activity changes both within and between runs for carbon monoxide oxidation (*7*). During runs several plateaux appeared which were related to the variable valence of samarium oxide, and between runs the change in activity was related to oxygen mobility (*8*).

0021-9517/78/0552-0166$02.00/0

Winter (*9, 10*) observed that nitrous oxide decomposition was not retarded by the addition of oxygen, whereas nitric oxide decomposition was retarded. This was explained by stating that nitrous oxide was adsorbed onto special sites which were not accessible to oxygen and that the $R_2$ centers, which resulted from nitrous oxide decomposition and which could accommodate auxiliary oxygen, were immediately destroyed.

The hydrogen–oxygen reaction has been studied in a large excess of hydrogen or oxygen at $7 \times 10^4$ $N$ $m^{-2}$ and 600 to 800 K on a catalyst pretreated by the gas in excess (*11*). The activation energy is 280 kJ $mol^{-1}$ in excess oxygen and 60 kJ $mol^{-1}$ in excess hydrogen. The activity is markedly decreased in excess hydrogen if the run is not preceded by hydrogen pretreatment. The stoichiometric reaction has also been studied on a sample heated in air and *in vacuo*, giving an activation energy of 48 kJ $mol^{-1}$, identical to that for oxygen exchange (*2, 4*). This leads to the conclusion that oxygen mobility is a critical factor in this reaction and that the rate-limiting step involves the interaction of molecular surface hydrogen with surface oxygen.

Two reactions which have been studied involving only hydrogen are parahydrogen conversion (*12*) and hydrogen adsorption (*13*). In a strong magnetic field nondissociative parahydrogen conversion shows an increase in activity, whereas there is a decrease in activity in a weak field. In the temperature range 77 to 99 K very low coverages of physically adsorbed hydrogen were detected, with a heat of adsorption of 8 kJ $mol^{-1}$ at 500 $N$ $m^{-2}$.

## EXPERIMENTAL METHODS

The apparatus and experimental procedure were identical to those described in a previous paper in this series (*14*). The catalyst was specpure grade samarium oxide (Johnson, Matthey) with a surface area of $3.5 \times 10^3$ $m^2$ $kg^{-1}$ and a total weight of $4.45 \times 10^{-4}$ kg. The structure, composition, and surface species were investigated using X-ray fluorescence, powder diffraction, and ir analysis.

Each reaction is identified by two numbers and a letter. The first number indicates the group of experiments conducted at an approximately constant temperature; the central letter indicates the set of experiments within the group, each set having a common initial hydrogen to oxygen ratio; and the final number indicates the run within the set, the total initial pressure usually changing for each separate run. Thirty-one groups of experiments were conducted.

All conditioning involved evacuation at $<10^{-4}$ $N$ $m^{-2}$, except for three sets of experiments in group 31, in which the catalyst was pretreated in hydrogen, oxygen, and air. The fresh catalyst was heated for 6 days at 773 K, and, prior to each group and most sets of reactions, the catalyst was heated at the reaction temperature for several hours. There was a 10-min evacuation time before each run. It should be noted that in the stoichiometric runs, 8Al-2, 9Al-2, and 15Al-3, the stoichiometric mixture had not reached equilibrium prior to admission onto the catalyst. In addition there was a slight air pretreatment prior to runs 18A2, 22A1, and 24A8. The system was calibrated initially and then prior to runs 2A1, 22A1, 30A1, and 31S1.

Groups 1 to 21 contain stoichiometric reactions at various temperatures in the range 323 to 558 K at an approximately constant initial hydrogen pressure of 220 $N$ $m^{-2}$, each group containing from 2 to 12 separate runs. Groups 22 to 27 contain stoichiometric reactions at 525, 467, 402, 329, 591, and 654 K, respectively, over the initial hydrogen pressure range 40 to 810 $N$ $m^{-2}$, approximately eight runs being conducted at each temperature. The nonstoichiometric reaction was studied at four different temperatures, 500, 589, 650, and 423 K, in groups 28 to 31, respectively, as summarized in Table 1. Also included in these groups are approximately 80 standard stoichiometric runs, usually at an initial hydrogen pressure of approximately 200 $N$ $m^{-2}$, their presence being indicated by missing letters in Table 1.

An IBM 370 computer was used in the analysis of the data, the reaction rates being determined by cubic spline interpolation. An IBM 2741 communication terminal was used to recall and plot the previously stored data (time, partial pressures, and log(-rate) at a specific temperature).

## RESULTS

### *Structure of Samarium Oxide*

Samarium oxide can exist in the *A* (hexagonal), *B* (monoclinic) or *C* (cubic) form, depending on temperature and environment; see, for example, (*15–20*). In general, samarium oxide exists in the *B* form above 1000 K (especially under reducing conditions) and in the *C* form at lower temperatures. There is some evidence that the *C* form is metastable and that the conversion from *C* to *B* with increasing temperature is irreversible. Samarium oxide readily absorbs water from the atmosphere and there is some evidence for the formation of hydrates of composition $3Sm_2O_3 \cdot 2H_2O$ and $3Sm_2O_3 \cdot H_2O$ which do not dehydrate until 1400 K (*20, 21*). However, analysis indicated that the catalyst used in the present work was *C* type with a space group $Ia3$ ($T_h{}^7$) and that water and hydroxyl groups have been removed by high-temperature vacuum conditioning.

McGough and Houghton (*22*) have investigated the effect of crystal structure on the reactivity of samarium oxide toward the dehydrogenation of cyclohexane and observed no difference in activity between the *B* and *C* types.

### *Analysis of Data*

The data were analyzed as before (*14*) and are summarized for nonstoichiometric reactions in Table 1. The initial rates are recorded directly after the cubic spline interpolation, and the initial pressures are determined independently by the capacitance manometer and by the McLeod gauge. The overall order with respect to time is obtained from the most linear section of the log(rate) vs log(pressure) plots, the pressure of the minor gas component being used in nonstoichiometric runs. The orders with respect to concentration are calculated from the initial rate data. The data were also analyzed by drawing isobaric curves through the log(rate) vs log(partial pressure) plots for nonstoichiometric reactions. These results are summarized in Tables 2 and 3.

The results of Group 25 were not analyzed because the rate was very low at 329 K, and, also, there had been a very slight air pretreatment prior to this group.

Three shapes for the log(rate) vs log(pressure) plots are identified as illustrated in Fig. 1. When these can be identified they are listed in Table 1.

### *Summary of the Results for the Stoichiometric Reactions*

*Reaction type.* Most of the reactions are of type a. Type b occurs infrequently, usually at high temperatures (600–650 K) and high initial hydrogen pressures (700–800 $N$ $m^{-2}$) (for example, runs 26Al-2, 27Al-2). Type c occurs in the vicinity of 400 K at medium pressures ($\sim$200 $N$ $m^{-2}$), and at higher temperatures with higher pressures.

*Catalyst activity.* The initial rates, and the rate of reaction of the central linear portion of each run, have been calculated, although they are not included in this paper.

The initial rate is fairly constant at 1 to 2 $N$ $m^{-2}$ $sec^{-1}$ in groups 1 to 21, with a

TABLE 1

Summary of the Experiments and Results for the Nonstoichiometric Hydrogen–Oxygen Reaction on Samarium Oxide

| Group, sets, and runs | Average temperature (K) | Initial $H_2$ pressure range ($N\ m^{-2}$) | Initial $H_2$–$O_2$ ratio | Average order with respect to time | | Reaction type |
|---|---|---|---|---|---|---|
| | | | | $O_2$ | $H_2$ | |
| 28B1-2 | 500 | 360, 160 | 2.25 | 0.3 | | a |
| 28D1-2 | | 280, 160 | 1.74 | | 0 | a |
| 28F1-2 | | 400, 160 | 2.50 | 0.26 | | a |
| 28I1-2 | | 240, 160 | 1.51 | | 0 | a |
| 28K1 | | 150 | 0.99 | | 1.3 | — |
| 28M1-2 | | 140, 70 | 0.50 | | 1.5 | c |
| 28O1-2 | | 440, 170 | 3.00 | 0.36 | | a |
| 28Q1-2 | | 160, 37 | 0.25 | | 1.5 | c |
| 28R1-2 | | 71, 22 | 0.14 | | 2.1 | a |
| 28T1-3 | | 1040, 150, 150 | 5.05 | 1 | | a |
| 28U1-3 | | 1030, 160, 160 | 5.99 | 1.4 | | a |
| 28W1-3 | | 160, 180 | 6.97 | 1.5 | | c |
| 28X1 | | 160 | 10.1 | 3.5 | | c |
| 29B1-2 | 589 | 360, 150 | 2.23 | 0.2 | | a |
| 29D1-2 | | 290, 150 | 1.76 | | 0 | a |
| 29F1-2 | | 400, 160 | 2.51 | 0.5 | | a |
| 29H1-2 | | — | 1.51 | | | |
| 29J1 | | 150 | 0.99 | | 1.3 | a |
| 29L1-2 | | 160, 76 | 0.50 | | 1.7 | a |
| 29N1-2 | | 480, 160 | 2.95 | 0.6 | | a |
| 29P1-2 | | 160, 36 | 0.25 | | 1.4 | a |
| 29Q1-2 | | —, 22 | 0.14 | | 2.1 | a |
| 29S1-2 | | 860, 160 | 4.99 | 1.1 | | c |
| 29T1-2 | | 970, 160 | 6.00 | 1.1 | | c |
| 29V1-2 | | —, 150 | 6.90 | 1.1 | | c |
| 29W1 | | 150 | 10.0 | 1.3 | | c |
| 30B1-2 | 650 | 360, 160 | 2.26 | 0.3 | | a |
| 30D1-2 | | 300, 170 | 1.70 | | 0 | a |
| 30F1-2 | | 430, 170 | 2.50 | 0.3 | | a |
| 30H1-2 | | — | 1.49 | | | |
| 30J1 | | 160 | 1.00 | | 1.3 | a |
| 30L1-2 | | 170, 80 | 0.50 | | 1.7 | a |
| 30N1-2 | | 520, 170 | 3.00 | 0.6, 1.5 | | a, c |
| 30P1-2 | | 170, 39 | 0.25 | | 1.3 | a |
| 30Q1-2 | | —, 23 | 0.14 | | 2.1 | a |
| 30S1-2 | | 920, 170 | 4.99 | 1.1 | | a, c |
| 30T1-2 | | >1000, 180 | 5.93 | 1.3 | | c |
| 30V1-2 | | —, 180 | 6.98 | 1.2 | | c |
| 30W1 | | 174 | 10.2 | 1.6 | | c |
| 31B1-2 | 423 | 380, 170 | 2.25 | 0.5 | | a |
| 31D1-2 | | — | 1.80 | | | |
| 31F1-2 | | 420, 170 | 2.49 | 0.4 | | a |
| 31H1-2 | | — | 1.49 | | | |
| 31J1 | | 340 | 1.00 | | 0 | a |
| 31L1-2 | | 170, 83 | 0.50 | | 1.6 | a |
| 31N1-2 | | 520, 170 | 3.06 | 0.6, 0.7 | | a, c |
| 31P1-2 | | 170, 39 | 0.25 | | 2.4 | c |

TABLE 2

Summary of the Average Reaction Rates ($N\ m^{-2}\ sec^{-1}$) for the Nonstoichiometric Groups 28, 29, and 30

| Initial hydrogen–oxygen ratio | Group 28 (500 K) | | Group 29 (589 K) | | Group 30 (650 K) | |
|---|---|---|---|---|---|---|
| | Excess of hydrogen | Excess of oxygen | Excess of hydrogen | Excess of oxygen | Excess of hydrogen | Excess of oxygen |
| 2.25 or 1.75 | 0.50<br>B[a] | 0.68<br>D | 0.55<br>B | 0.70<br>D | 0.53<br>B | 0.84<br>D |
| 3.00 or 1.00 | 0.47<br>F | 0.74<br>I | 0.50<br>F | 0.79<br>H | 0.45<br>F | 0.84<br>H |
| 5.00 or 0.25 | 0.089<br>U | 0.056<br>Q | 0.16<br>S | 0.050<br>P | 0.070<br>S | 0.060<br>L |
| 7.00 or 0.14 | 0.03<br>W | 0.019<br>R | 0.05<br>V | 0.01<br>Q | 0.06<br>S | 0.02<br>L |

[a] Set from which the rates are taken.

constant initial pressure and varying temperature. The first run on the fresh catalyst gave an abnormally high rate. The initial rate increases to 2 to 3 $N\ m^{-2}\ sec^{-1}$ when both the initial pressure and the temperature are high (for example, groups 22, 26, and 27). Runs preceded by excess hydrogen or oxygen have a slightly reduced initial activity, with hydrogen excess having the greater effect.

The rate of the central linear portion is relatively constant between 0.4 and 0.6 $N\ m^{-2}\ sec^{-1}$, with a tendency to increase with increasing temperature or pressure. There is no obvious pretreatment effect on this rate, even for sets 31R, 31T, and 31U after the catalyst had been baked in hydrogen, oxygen, and air, respectively.

The time taken for the reactions to go to completion is fairly consistent throughout the constant initial pressure temperature-dependent runs, taking about 500 to 600 sec for 95% completion.

*Orders with respect to time.* The orders

TABLE 3

Average Slopes and Maxima from the Isobars

| Isobar | Group | Temperature (K) | Hydrogen to oxygen ratio at maximum of isobar | Standard deviation | Slope of isobar | | | |
|---|---|---|---|---|---|---|---|---|
| | | | | | Low-pressure side of isobar | Standard deviation | High-pressure side of isobar | Standard deviation |
| Hydrogen | 28 | 500 | 1.03 | 0.099 | 1.08 | 0.13 | −1.22 | 0.08 |
| Hydrogen | 29 | 589 | 1.18 | 0.23 | 1.30 | 0.25 | −1.06 | 0.23 |
| Hydrogen | 30 | 650 | 1.08 | 0.15 | 1.18 | 0.26 | −0.99 | 0.18 |
| Hydrogen | 31 | 423 | 0.97 | 0.18 | 1.20 | 0.15 | −1.89 | 0.31 |
| Oxygen | 28 | 500 | 1.05 | 0.13 | 1.39 | 0.28 | −1.02 | 0.24 |
| Oxygen | 29 | 589 | 1.11 | 0.40 | 1.28 | 0.26 | −1.08 | 0.22 |
| Oxygen | 30 | 650 | 1.24 | 0.23 | 1.20 | 0.37 | −0.99 | 0.11 |
| Oxygen | 31 | 423 | 1.02 | 0.10 | 2.09 | 0.67 | −1.18 | 0.44 |

with respect to time are calculated from the central linear portion of each plot. In most cases this section starts after about 10% of the reaction has occurred and continues for the next 80%. Most of the reactions are in the range 0 to 0.1 order. There is no obvious temperature dependence, but a trend toward slightly higher orders at low initial pressures. For runs 22A8, 23A7, 24A8, 27A9, and 28G1, all at very low initial hydrogen pressures of 40 to 50 *N* $m^{-2}$, the plots are very erratic, often giving very high orders for some sections of the curve.

*Orders with respect to concentration.* These orders are calculated from the five pressure-dependent groups, 22 to 27 (excluding group 25). The orders obtained were 0.3, 0.2, 0.5, 0.5, and 0.7 at 402, 467, 525, 591, and 654 K, respectively. Therefore, there is a tendency toward higher orders at higher temperatures.

*Temperature effects.* Some of these effects have already been mentioned in the sections above. The Arrhenius plot, assuming zero-order kinetics, is shown in Fig. 2. The activation energy changes with temperature, from a value of about 7 kJ $mol^{-1}$ at 350 K to 1 kJ $mol^{-1}$ at 400 K.

### *Summary of the Results for the Nonstoichiometric Reactions*

*Reaction type.* The reaction type is less easily classified than for stoichiometric reactions but usually one type predominates, as shown in Table 1. Most reactions are type a, especially when the initial hydrogen–oxygen ratio is close to 2. There is a tendency toward type c at high ratios. Type c also occurs at low ratios when the temperature is low, especially if the initial pressure is also low. No type b plots occur. The most regular and consistent results are obtained in excess hydrogen or at high temperatures.

*Catalytic activity.* The initial rate decreases as the hydrogen–oxygen ratio becomes more extreme (that is, as either hydrogen or oxygen are in large excess), down to about 0.1 *N* $m^{-2}$ $sec^{-1}$, with the rate usually being higher in oxygen excess than in hydrogen excess.

The average rates for the major portion of the reaction are summarized in Table 2

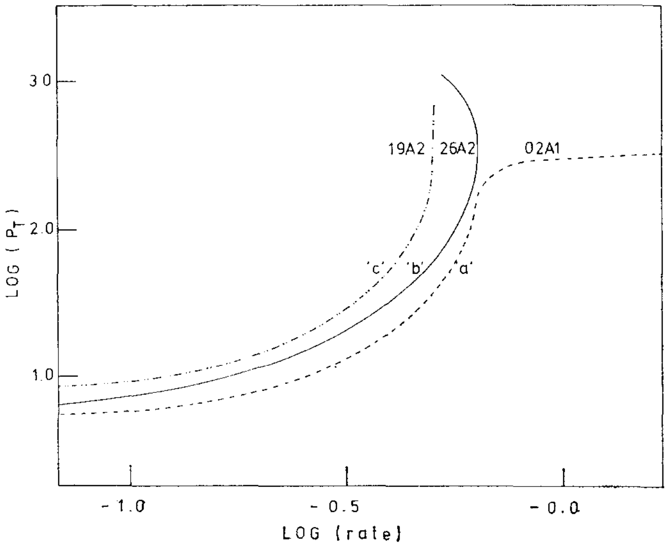

FIG. 1. Typical features of the three types of log(rate) vs log(pressure) plots. Reaction 02A1 is type a, reaction 26A2 is type b, and reaction 19A2 is type c.

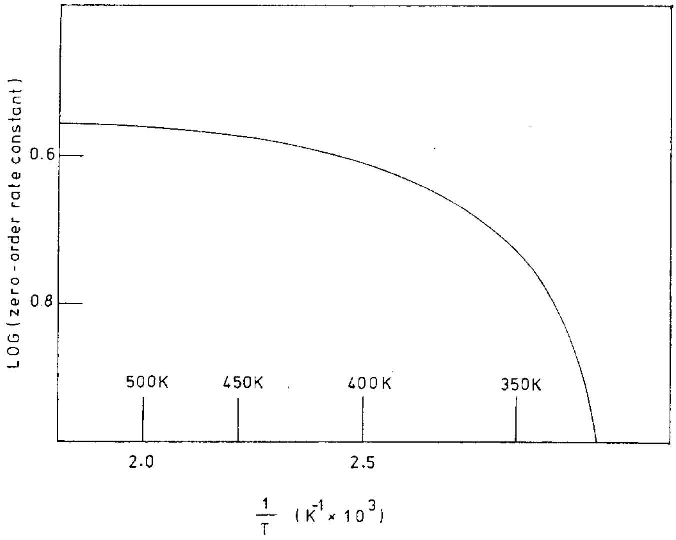

FIG. 2. Arrhenius plot from the results of groups 01 to 21.

for groups 28 through 30. For hydrogen–oxygen ratios close to stoichiometry (that is, ratios from 1.00:1 to 3.00:1) the rates in excess hydrogen are very similar. The rates in excess oxygen are slightly higher and increase with temperature. For more extreme ratios, the rates decrease significantly, and the rate in oxygen excess is now lower than the rate in hydrogen excess.

*Orders with respect to time.* As can be seen from Table 1, the orders with respect to time increase as the hydrogen–oxygen ratio becomes more extreme. The order in hydrogen increases up to 2.1 (except for a value of 2.4 in set 31P), and the order in

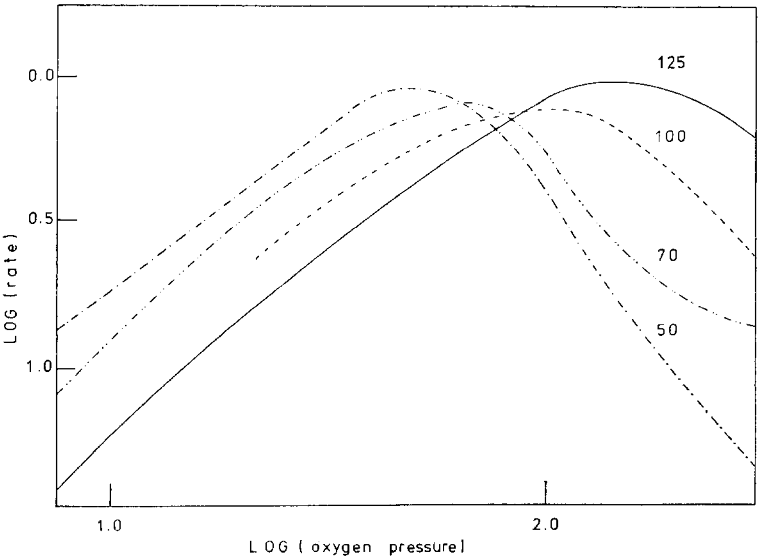

FIG. 3. Hydrogen isobars at 500 K from group 28. The constant hydrogen pressures are shown in Newtons per square meter.

oxygen increases up to 1.6 (except for a value of 3.5 in set 28×).

*Isobar.* For all four nonstoichometric groups the hydrogen and oxygen isobars exhibit maxima. The results are summarized in Table 3, and typical isobars are shown in Fig. 3 and 4.

The ratio at the maxima of the isobars decreases with increasing oxygen pressure and increases with increasing hydrogen pressure. Also, in general, the ratio increases with increasing temperature.

The slopes on either side of the maxima do not show any obvious pattern with changing pressure, but do tend to decrease with increasing temperature. The absolute value of the average slope from the low-pressure side of the hydrogen isobar and the high-pressure side of the oxygen isobar is 1.3, and the average value of the opposite slopes is 1.5. However, the error is very large. By neglecting the average values from Table 3, where the standard deviation is greater than 0.3, the first average slope reduces to 1.1 ± 0.2 and the second to 1.2 ± 0.1.

## DISCUSSION

The overall results fit the general pattern described for dysprosium oxide (*23*). The general characteristics of the results will be discussed, a kinetic expression will be presented, and a mechanism will be proposed.

### *General Characteristics*

*Reaction type.* Most of the reactions are of type a, involving a large decrease in the rate at the beginning of the reaction. Other workers (see the Introduction) have shown that the surface of samarium oxide is very sensitive to reaction conditions, and that pretreatment by, or exposure to, oxygen (particularly below about 450 K) reduces the activity by decreasing the number of active sites. It is probable, therefore, that the first section of the type a plots is the result of reversible deactivation of the most active sites. This type is less predominant at high hydrogen–oxygen ratios and is seen less often at high temperatures, both facts supporting the idea of oxygen deactivation. The appearance of type b at

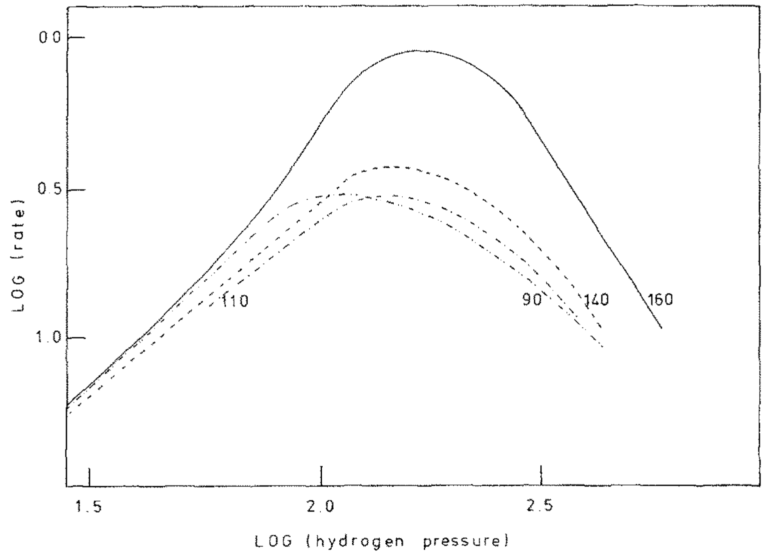

FIG. 4. Oxygen isobars at 650 K from group 30. The constant oxygen pressures are shown in Newtons per square meter.

high temperatures indicates that the adsorption sites are not immediately available, resulting in a delay before equilibrium is established.

*Catalyst activity.* The initial rate (which is related to reaction type) is not significantly temperature dependent below 500 K, indicating that the most active sites are readily available at these temperatures. However, there is a slight decrease in the initial rate above 500 K. Excess of hydrogen or oxygen (or prior exposure to nonstoichiometric reactions) reduces the initial rate, due to partial deactivation of the active sites. Pretreatment with hydrogen, or reactions with hydrogen excess, have a slightly lower initial rate than those involving oxygen.

The rate of the central linear portion does not show any effect of pretreatment, giving further evidence for the existence of a small number of very active sites which are readily deactivated at the start of the reaction. As the hydrogen–oxygen ratio becomes more extreme, the rate decreases, due to an excess of one of the gases on the surface. The fact that the rate in oxygen excess is lower than the rate in hydrogen excess suggests that the active sites are more readily deactivated by oxygen than by hydrogen.

The change in activity with temperature is illustrated by the Arrhenius plot (Fig. 2), showing a very low activation energy above temperatures at which the oxygen mobility becomes significant (*5*).

*Active sites.* At least two sets of active sites have been described: a hyperactive set, characterized by the reaction type, the initial rates, and the orders with respect to concentration; and a less active set, characterized by the rates of the central portions of the plots, and the orders with respect to time.

From previous studies on samarium oxide, other lanthanide oxides, and similar oxides (for example, (*24, 25*)), at least two classes of sites can be identified. One results from the loss of hydroxyl groups during conditioning, and the other results from loss of surface oxygen, or anion vacancies inherent in the structure (for example, (*7, 19, 26*)). The first class of sites can exist in varying forms with differing activity (*25*), and the second class of sites is probably predominant and can give rise to *n*-type semiconductivity at low oxygen pressures (*26*).

It is possible that the hyperactive set of sites belongs to the first class. This would explain the lack of temperature dependence which would have been expected if the sites were associated with anion vacancies and therefore susceptible to changes in oxygen mobility with temperature (*5*). The appearance of type b, and the slight decrease in initial rate at temperatures approaching the conditioning temperature, would be expected, as would the greater deactivating effect of hydrogen over oxygen. The orders with respect to concentration indicate that there may be some dissociative adsorption occurring on these sites, and again, this would be very likely on the adjacent sites produced by loss of hydroxyl groups.

The less active sites are probably associated with the second class of sites. This is supported by the similarity between the rate of the hydrogen–oxygen reaction and the oxygen exchange reaction, and the conclusion that oxygen mobility is a critical factor in both reactions (*2, 4*). Oxygen has a greater deactivating effect than hydrogen, and the activation energy in excess oxygen is much higher than that in excess hydrogen (*11*). Most of the reaction occurs on these sites and the kinetics and mechanism which follow describe this portion of the results.

### *Kinetic Expression*

From the similarity between the results for samarium oxide and those already described for dysprosium oxide (*23*), a general kinetic expression can be proposed, namely,

$$-\frac{dP_T}{dt} = \frac{k(b_{H_2}P_{H_2})^x(b_{O_2}P_{O_2})^y}{(1 + b_{H_2}P_{H_2} + b_{O_2}P_{O_2})^{x+y}}, \quad (1)$$

where $k$ is a proportionality constant, $b_{H_2}$ and $b_{O_2}$ are the adsorption coefficients for hydrogen and oxygen, respectively, and $x$ and $y$ are integers. The results will now be discussed in terms of this relationship.

*Orders with respect to time.* Most of the orders for the stoichiometric reactions are close to zero. This is to be expected if Eq. (1) is obeyed and if $((2b_{H_2} + b_{O_2})/3)P_T > 1$, where $P_T$ is the total pressure of hydrogen plus oxygen. Further evidence for this is obtained from the higher orders at very low pressures.

The individual orders with respect to hydrogen or oxygen can be obtained from the log (rate) vs log (pressure minor component) plot, assuming that the other gas is sufficiently in excess for its concentration to be considered constant. The results shown in Table 1 indicate an order for both hydrogen and oxygen of between 1 and 2, with hydrogen being closer to 2 and oxygen closer to 1.

*Isobars.* The maxima observed in all the isobars indicates that there is competitive adsorption, as shown by other results and incorporated into Eq. (1). The positive slope of the hydrogen isobar and the negative slope of the oxygen isobar give a value for $y$, and vice versa for $x$. The oxygen order varies considerably, but if results are omitted for slopes corresponding to anomalous values for the isobaric maxima a value close to 1 is obtained. In general, higher values are obtained for the hydrogen order but the evidence is not sufficiently conclusive to determine whether the order is 1 or 2 or some intermediate value.

TABLE 4

Average Values for the Adsorption Coefficients with $x = 1$, $y = 1$

| Group number | Temperature (K) | Oxygen pressure range ($N\ m^{-2}$) | Constant partial pressure | $b_{O_2} \times 10^2$ ($N^{-1}\ m^2$) | $b_{H_2} \times 10^2$ ($N^{-1}\ m^2$) |
|---|---|---|---|---|---|
| 31 | 423 | 130–170 | $H_2$ | 0.5 | 0.2 |
| | | 140–160 | $O_2$ | 0.2 | 0.8 |
| 28 | 500 | 54–70 | $H_2$ | 3.5 | 1.5 |
| | | — | — | — | — |
| 29 | 589 | — | — | — | — |
| | | 85–140 | $O_2$ | 0.2 | 0.8 |
| 30 | 650 | 52–100 | $H_2$ | 3.7 | 1.7 |
| | | 90–140 | $O_2$ | 0.3 | 1.0 |

The hydrogen–oxygen ratio at the maxima of the isobars is relatively constant, with most being in the range 1.0 ± 0.1. From Eq. (1) the maxima should obey the following equations:

Hydrogen isobar, $x = y = 1$,

$$\frac{P_{H_2}}{P_{O_2}} = \frac{b_{O_2}P_{O_2} - 1}{b_{H_2}P_{O_2}}, \quad (2)$$

$x = 2$, $y = 1$,

$$\frac{P_{H_2}}{P_{O_2}} = \frac{2b_{O_2}P_{O_2} - 1}{b_{H_2}P_{O_2}}, \quad (3)$$

Oxygen isobar, $x = y = 1$,

$$\frac{P_{H_2}}{P_{O_2}} = \frac{b_{O_2}P_{O_2} + 1}{b_{H_2}P_{O_2}}, \quad (4)$$

$x = 2$, $y = 1$,

$$\frac{P_{H_2}}{P_{O_2}} = \frac{2b_{O_2}P_{O_2} + 2}{b_{H_2}P_{O_2}}. \quad (5)$$

The results, therefore, agree with the above equations, with an indication that $b_{H_2}$ and $b_{O_2}$ may be changing slightly with pressure and temperature. The decrease in the ratio at the maxima with an increase in oxygen pressure could be explained by a decrease in $b_{O_2}$ as a result of occupation of more active sites by oxygen. Similarly, the increase in the ratio with an increase in hydrogen pressure could be the result of a decrease in $b_{H_2}$.

In Table 4 average values for $b_{O_2}$ and $b_{H_2}$ are calculated from Eqs. (2) and (4)

TABLE 5

Average Values for the Adsorption Coefficients with $x = 2$, $y = 1$

| Group number | Temperature (K) | Oxygen pressure range ($N\ m^{-2}$) | Constant partial pressure | $b_{O_2} \times 10^2$ ($N^{-1}\ m^2$) | $b_{H_2} \times 10^2$ ($N^{-1}\ m^2$) |
|---|---|---|---|---|---|
| 31 | 423 | 130–170 | $H_2$ | 0.5 | 0.5 |
| | | — | — | — | — |
| 28 | 500 | 50–70 | $H_2$ | 1.5 | 1.7 |
| | | — | — | — | — |
| 29 | 589 | 20–80 | $H_2$ | 6 | 7 |
| | | 80–120 | $H_2$ | 1 | 1.5 |
| | | 85–130 | $O_2$ | 0.2 | 1.6 |
| 30 | 650 | 50–70 | $H_2$ | 1.7 | 1.5 |
| | | 90–130 | $O_2$ | 0.2 | 1.2 |

From the hydrogen isobars, $b_{O_2}$ and $b_{H_2}$ show an increase with temperature, with $b_{O_2} > b_{H_2}$ at any particular temperature. From the oxygen isobars, there is no change with temperature, but in this case $b_{O_2} < b_{H_2}$. The values of $b_{H_2}$ from the two isobars agree within an order of magnitude, but the values of $b_{O_2}$ are significantly lower using Eq. (4) than using Eq. (2).

In Table 5 average values for $b_{O_2}$ and $b_{H_2}$ are calculated from Eqs. (3) and (5). Both adsorption coefficients increase from 423 to 500 K and then remain effectively constant. The values for $b_{H_2}$ calculated from both the oxygen and the hydrogen isobars are similar, but the value of $b_{O_2}$ is lower using Eq. (5) than using Eq. (3). However, at 589 K, $b_{O_2}$ decreases with increasing oxygen pressure, and, therefore, since the oxygen pressure range is higher when using Eq. (5) rather than Eq. (3), lower values for $b_{O_2}$ would be expected. In addition, it should be pointed out that the values for $b_{O_2}$ are calculated using fewer data points than were used to calculate $b_{H_2}$. The change in the values of the adsorption coefficients in the vicinity of 400 to 500 K might be expected in view of the change in oxygen mobility affecting the heat of adsorption, or it may just be a pressure effect resulting from the high-pressure range in group 31.

In general, a relatively constant value for $b_{O_2}$ and $b_{H_2}$ of approximately $1.5 \times 10^{-2}$ $N^{-1}\ m^2$ is obtained at oxygen pressures in the vicinity of 100 $N\ m^{-2}$. Substitution of these values into Eq. (1) for stoichiometric mixtures leads to a denominator of $(1 + 1.5 \times 10^{-2} P_T)^{x+y}$. For reactions with an initial hydrogen pressure of 200 $N\ m^{-2}$, the denominator equals $(1 + 4.5)^{x+y}$, which will give close to zero-order kinetics. A slight increase in order with decreasing pressure would be expected. Comparing the results in Tables 4 and 5 it appears that a more logical pattern is developed with $x = 2$, $y = 1$ than with $x = y = 1$.

A value for the proportionality constant, $k$, has been calculated using the average values for $b_{O_2}$ and $b_{H_2}$ of $1.5 \times 10^{-2}$ $N^{-1}\ m^2$. The values calculated at five different temperatures are shown in Table 6, for $x = y = 1$ and for $x = 2$, $y = 1$. Both sets of results give a relatively constant value for $k$ from the central portion of the reaction (though a slight increase with time is detected) and show little temperature dependence except between the lowest two temperatures.

From a consideration of all of the kinetic data it is concluded that $y = 1$ and that the most likely value for $x$ is 2.

### *Mechanism*

From previous results for the stoichiometric reaction, and the nonstoichiometric reaction in a large excess of hydrogen or

TABLE 6

Values for the Proportionality Constant $k$ ($N\ m^{-2}\ sec^{-1}$)

| Reaction | Temperature (K) | Proportionality constant | |
|---|---|---|---|
| | | $x = 1$, $y = 1$ | $x = 2$, $y = 1$ |
| 19A2 | 377.5 | 4 | 8 |
| 02A1 | 488.9 | 5 | 10 |
| 13A1 | 505.4 | 5 | 9 |
| 01A9 | 515.0 | 5 | $9 \rightarrow 10$ |
| 26A2 | 592.0 | $3 \rightarrow 4$ | $5 \rightarrow 6$ |

oxygen, and from similarities between the hydrogen–oxygen reaction and the oxygen exchange reaction, it has been postulated that the rate-limiting step involves the interaction of molecular hydrogen and surface oxygen (*2*, *4*, *11*). Also, it is known that hydroxyl groups form readily on the surface of samarium oxide, and it has already been proposed that certain of the active sites on the surface appear as a direct result of the loss of these groups. Therefore, the following general mechanism, already proposed for other lanthanide oxides (for example, dysprosium oxide (*23*)), and certain metals (for example, platinum and palladium (*27*)) is the most likely:

$$H_{2(g)} \rightleftarrows H_{2(ads)} \qquad (i)$$

$$O_{2(g)} \rightleftarrows O_{2(ads)} \qquad (ii)$$

$$H_{2(ads)} + O_{2(ads)} \rightleftarrows H_2O_{2(ads)} \qquad (iii)$$

$$H_2O_{2(ads)} + H_{2(ads)} \rightarrow 2H_2O_{(ads)} \qquad (iv)$$

$$H_2O_{(ads)} \rightleftarrows H_2O_{(g)} \qquad (v)$$

This mechanism will give rise to the kinetic expression shown in Eq. (1), with $x = 2$ and $y = 1$.

In conclusion, the present kinetic results indicate that there are at least two groups of active sites. The initial reaction takes place on a hyperactive group, which is readily, but reversibly, deactivated. This group may result from the loss of hydroxyl groups from the surface during conditioning. The bulk of the reaction takes place on the second group of less active but more stable sites, which are probably anion vacancies. The kinetics obey Eq. (1) with $y = 1$ and probably with $x = 2$. The mechanism is based on the scheme shown above in (i) through (v), with a rate-determining step of interaction between $H_2O_{2(ads)}$ (or, simply, two adjacent hydroxyl groups) and adsorbed hydrogen.

## ACKNOWLEDGMENT

The authors express their appreciation to the National Research Council and Shell (Canada) Ltd. for the financial support of this project.

## REFERENCES

*1.* Lowdermilk, F. R., and Day, A. R., *J. Amer. Chem. Soc.* **52**, 3535 (1930).
*2.* Minachev, Kh. M., *in* "Proceedings, 5th International Congress on Catalysis, Vol. 1, p. 219. 1973.
*3.* Hattori, T., Inoko, J., and Murakami, Y., *J. Catal.* **42**, 60 (1976).
*4.* Minachev, Kh. M., and Antoshin, G. V., *Dokl. Akad. Nauk. SSSR* **161**, 122 (1965).
*5.* Sokolovskii, V. D., Sazonov, L. A., Boreskov, G. K., and Moskvina, Z. V., *Kinet. Katal.* **9**, 784 (1968).
*6.* Winter, E. R. S., *J. Chem. Soc. A*, 1832 (1969).
*7.* Sazonov, L. A., and Logvinenko, M. G., *Kinet. Katal.* **3**, 761 (1962).
*8.* Sazonov, L. A., Artamonov, E. V., and Mitrofanova, G. N., *Kinet. Katal.* **12**, 378 (1971).
*9.* Winter, E. R. S., *J. Catal.* **34**, 431 (1974).
*10.* Winter, E. R. S., *J. Catal.* **34**, 440 (1974).
*11.* Bakumenko, T. T., *Kinet. Katal.* **6**, 74 (1965).
*12.* Selwood, P. W., *J. Catal.* **22**, 123 (1971).
*13.* Read, J. F., *Canad. J. Chem.* **50**, 490 (1972).
*14.* Read, J. F., Dunfield, L. G., Shreve, R. M., and Spinney, E. A., *J. Catal.* **33**, 335 (1974).
*15.* Cromer, D. T., *J. Phys. Chem.* **61**, 753 (1957).
*16.* Roth, R. S., and Schneider, S. J., *J. Res. Nat. Bur. Std. A* **64**, 309 (1960).
*17.* Warshaw, I., and Roy, R., *J. Phys. Chem.* **65**, 2048 (1961).
*18.* Eyring, L., and Holmberg, B., *Advan. Chem.* **39**, 46 (1963).
*19.* Boganov, A. G., and Rudenko, V. S., *Dokl. Akad. Nauk. SSSR* **161**, 590 (1965).
*20.* Dean, J. R., and Bloor, D., *J. Phys. C* **5**, 1237 (1972).
*21.* Glushkova, V. B., and Koehler, E. K., *Mater. Res. Bull.* **2**, 503 (1967).
*22.* McGough, C. B., and Houghton, G., *J. Phys. Chem.* **65**, 1887 (1961).
*23.* Read, J. F., and Perkins, E. W., *J. Catal.* **42**, 443 (1976).
*24.* Read, J. F., and Perkins, E. W., *J. Catal.* **42**, 455 (1976).
*25.* Peri, J. B., *J. Catal.* **41**, 227 (1976).
*26.* Subba Rao, G. V., Ramdas, S., Mehrotra, P. N., and Rao, C. N. R., *J. Solid State Chem.* **2**, 377 (1970).
*27.* Tret'yakov, I. I., Sklyarov, A. V., and Shub, B. R., *Kinet. Katal.* **11**, 479 (1970).